

as the original CD measurements³ (also at pH 7.4) and extended their range to lower temperature to produce a more complete picture of its thermal stability. We report these results below along with comparisons that can be made without recourse to the theory for two-chain molecules. A detailed fit of these data to the latter theory is in progress and will occupy some time, so comments on that will not be attempted here.

Materials and Methods

Preparation of α -tropomyosin from rabbit cardiac muscle and manipulation of both proteins were as previously described.³ The β -tropomyosin was obtained from rabbit skeletal tropomyosin by ion exchange chromatography;¹¹ no α -chains appeared on polyacrylamide gel electrophoresis in the presence of sodium dodecyl sulfate. Circular dichroism measurements were made with the same precautions with respect to temperature measurement and control, base line monitoring, and reversibility as before.³ Calculation of fraction helix from CD was also as previously described.³ All measurements were on non-cross-linked protein; i.e., the samples were reduced with dithiothreitol (DTT) and kept in solutions containing protective amounts of DTT. In all cases the medium is $(\text{NaCl})_{500}(\text{NaP}_i)_{50}(\text{DTT})_x(7.4)$,¹² with $0.5 \leq x \leq 1$ mM. The complete reversibility observed makes clear that no cross-linking occurred by air oxidation during the somewhat lengthy thermal denaturation determinations. As an added check, we measured a few freshly reduced samples after rapidly bringing them to an elevated temperature. These results agreed well with those recorded at the same elevated temperature in the routine protocol.

In an investigation in which absolute values of helix content for two different proteins are to be compared, it is essential to be sure that determinations of protein concentrations are accurate. In this laboratory, we have for some years employed absorbance at 277 nm to determine tropomyosin concentration with a numerical value of $0.314 \text{ cm}^2 \text{ mg}^{-1}$ for the extinction coefficient, a value originally determined with rabbit skeletal tropomyosin through micro-Kjeldahl determinations of nitrogen content.¹³ Since α -tropomyosin and β -tropomyosin have the same number of tyrosines per molecule, nearly the same molecular weight, and nearly the same conformation, it would seem likely that the same value could be used for them as for the skeletal protein, which is an almost equimolar mixture of $\alpha\alpha$ and $\alpha\beta$ species. Nevertheless, to justify this routine use of the same extinction coefficient for all our tropomyosin samples, we checked our concentration measurement using the method of Edelhoch.¹⁴

In Edelhoch's method, the tyrosine concentration is determined by dissolving the protein in denaturing medium (6 M guanidinium chloride (GdmCl)) buffered at pH 6.5 and recording the change in absorbance (at 295 nm) resulting from titration to pH 12.5. The method is useful because essentially only tyrosines titrate in that pH range and the change in tyrosine extinction coefficient at 295 nm is very large, has been accurately measured, and is the same for all proteins in the unfolded state.¹⁴ Since the tyrosine content of both α - and β -tropomyosin is well-known,⁶ the protein concentration can easily be calculated from the data.

In the present context, the absorbance (277 nm) of a reduced protein solution in benign medium, $(\text{KCl})_{500}(\text{KP}_i)_{50}(7.4)$, was measured and the "routine" protein concentration calculated by our usual method. A 0.400-mL aliquot of this solution was then added to a 2.00-mL volumetric flask containing 1.50 mL of $(\text{GdmCl})_{800}(\text{KCl})_{250}(\text{KP}_i)_{25}(6.5)$. Dilution to the mark with water then provided a solution of the unfolded protein (at the proper pH) whose "routine" concentration could be deduced from its history and whose absorbance (295 nm) was measured. The volume of 45% KOH required to bring the solution to pH 12.5 was also known from a preliminary experiment, so that the absorbance (295 nm) measured after addition of base could be corrected for the small, additional dilution.¹⁵ Thus, the protein concentration deduced from our original routine absorbance method and from Edelhoch's method were compared. When this procedure was carried out on α - and β -tropomyosin, agreement between our routine value and the value from the Edelhoch method was within 2% for each protein. We conclude that use of absorbance at 277 nm with an extinction coefficient of 0.314

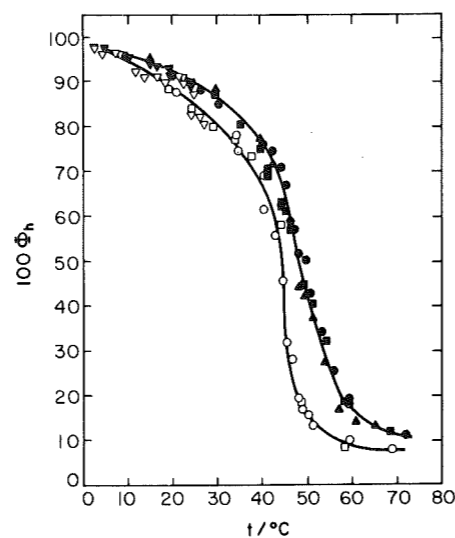


Figure 1. Percent helix vs. Celsius temperature for reduced α -tropomyosin in $(\text{NaCl})_{500}(\text{NaP}_i)_{50}(\text{DTT})_x(7.4)$. Filled symbols: 5.2 mg mL^{-1} , $x = 1.0$ mM. Open symbols: $0.0044 \text{ mg mL}^{-1}$, $x = 0.5$ mM. Various shaped symbols designate different runs. Solid curves are spline curves.

$\text{cm}^2 \text{ mg}^{-1}$ provides correct values for the concentration of both the α - and β -proteins.

The use of protein solutions as dilute as $0.0044 \text{ mg mL}^{-1}$ raises questions concerning adsorption of protein to the walls of the CD cells. The danger is that the adsorbed material may be an appreciable fraction of the total, thus reducing the effective concentration in the cell. We guard against this by rinsing the cell with the solution preliminary to loading the actual sample. However, we have never found any difference in CD between these solutions and those loaded directly into a dry cell. In the present instance, this effect is apparently immaterial.

Results and Discussion

Results of our augmented study of the thermal denaturation of α -tropomyosin are shown in Figure 1 for two extreme concentrations of protein. The spline curves through the data differ only slightly from our previous values because of the extension of the data to lower temperatures. The effect of protein concentration as previously observed is in evidence, although it is again apparent that careful temperature measurements and a wide range of concentration (for Figure 1, a 1200-fold concentration range) are required for its demonstration. This "mass action" effect must be caused by the dissociation of the two chains in the transition.

Corresponding data for β -tropomyosin over a slightly narrower range of concentration (500-fold) are shown in Figure 2. The results are qualitatively rather similar to the α -tropomyosin data. The concentration effect is clearly seen here as well, although the difference is somewhat less, almost certainly because the range is somewhat smaller. In neither reduced α - nor in reduced β -tropomyosin in the range 0–70 °C do we see evidence in our data for small transitions in addition to the principal transition, as has been reported for reduced skeletal tropomyosin (at ~ 7 °C)¹⁵ and reduced α -tropomyosin (at ~ 30 °C, and 1 M ionic strength).¹⁶

Comparison of the stability of the double α -helix in α_2 and in β_2 molecules is most directly made for comparable concentrations. Such a direct comparison is shown in Figure 3, where data for intermediate, almost identical concentrations of each protein are displayed. It is clear that the two-chain, α -helical, coiled coil is appreciably more stable in α_2 than in β_2 molecules. This conclusion has previously been reached, but only very limited data were

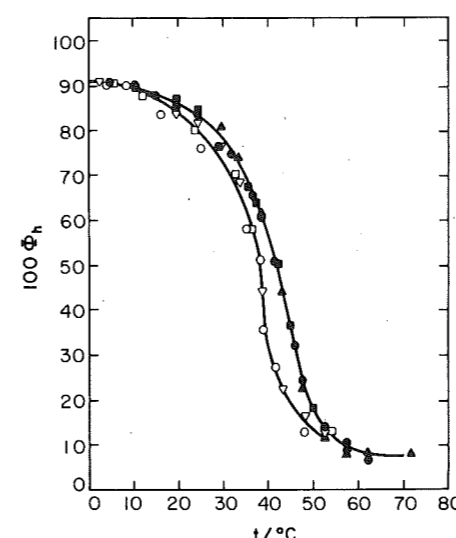


Figure 2. Percent helix vs. Celsius temperature for reduced β -tropomyosin in $(\text{NaCl})_{500}(\text{NaP}_i)_{50}(\text{DTT})_x(7.4)$. Filled symbols: 4.72 mg mL^{-1} , $x = 1.0$ mM. Open symbols: $0.0100 \text{ mg mL}^{-1}$, $x = 0.5$ mM. Various shaped symbols designate different runs. Solid curves are spline curves.

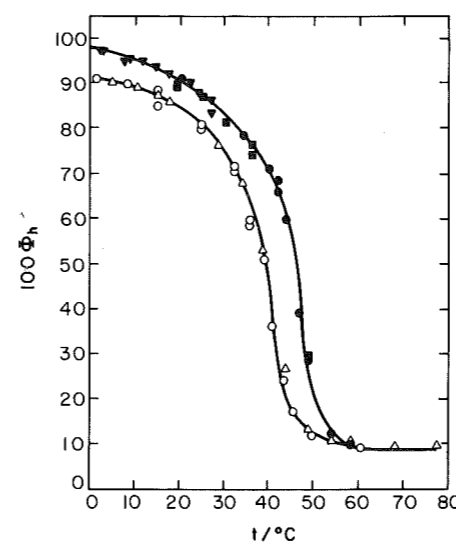


Figure 3. Percent helix vs. Celsius temperature for reduced tropomyosins in $(\text{NaCl})_{500}(\text{NaP}_i)_{50}(\text{DTT})_{0.5}(7.4)$. Filled symbols: α -tropomyosin at 0.104 mg mL^{-1} . Open symbols: β -tropomyosin at 0.100 mg mL^{-1} . Various shaped symbols designate different runs. Solid curves are spline curves.

presented to support it.¹⁷ The present more detailed study not only confirms this conclusion but provides a data base broad enough to support a detailed test of the theory of the α -helix-to-random-coil transition in these molecules.

In advance of an attempt to fit these data to the extant theory,¹⁰ it is premature to speculate on the results. However, one conclusion can be stated because it is independent of the two-chain theory. The observed difference in stability between α - and β -tropomyosin cannot result from differences in the short-range (σ and $s(T)$) interactions. We have been aware for some time that the helix content predicted from the helix-coil theory for single chains of α -tropomyosin and β -tropomyosin at 30 °C are almost identical.¹⁸ We have extended the same calculation to cover the entire experimentally accessible temperature range (0–80 °C) and find that predicted differences never exceed a fraction of a percentage point in helix content. It is thus immediately apparent (and dependent only on the theory for single chains) that observed differences between the thermal denaturation curves of the α_2 and β_2

molecules must arise from interactions other than those of short range. Whether these non-short-range differences are, in fact, the helix-helix interactions which are the only such interactions introduced in the two-chain theory,¹ whether the two-chain theory in its more complete form¹⁰ treats them correctly, and whether sense can be made of the observed differences in terms of the 39 out of 284 amino acid sites (11 of which are at the hydrophobic, helix-helix contact surface) at which α - and β -tropomyosin chains differ remain open questions.

Acknowledgment. This study was supported by Grant No. GM-20064 from the Division of General Medical Sciences, U.S. Public Health Service.

References and Notes

- (1) Skolnick, J.; Holtzer, A. *Macromolecules* 1982, 15, 303–314.
- (2) Skolnick, J.; Holtzer, A. *Macromolecules* 1982, 15, 812–821.
- (3) Holtzer, M. E.; Holtzer, A.; Skolnick, J. *Macromolecules* 1983, 16, 173–180.
- (4) Holtzer, M. E.; Holtzer, A.; Skolnick, J. *Macromolecules* 1983, 16, 462–465.
- (5) Skolnick, J.; Holtzer, A. *Macromolecules* 1983, 16, 1548–1550.
- (6) Mak, A.; Lewis, W.; Smillie, L. *FEBS Lett.* 1979, 105, 232–234.
- (7) Scheraga, H. *Pure Appl. Chem.* 1978, 50, 315–324.
- (8) Skolnick, J. *Macromolecules* 1983, 16, 1069–1083.
- (9) Skolnick, J. *Macromolecules* 1983, 16, 1763–1770.
- (10) Skolnick, J. *Macromolecules* 1984, 17, 645–658.
- (11) Cummins, P.; Perry, S. *Biochem. J.* 1973, 133, 765–777.
- (12) We describe complex aqueous solvent media by giving the chemical formula of each solute in parentheses with its millimolarity as subscript, followed by the pH in parentheses. Other abbreviations are as follows: DTT, dithiothreitol; CD, circular dichroism; GdmCl, guanidinium chloride.
- (13) Holtzer, A.; Clark, R.; Lowey, S. *Biochemistry* 1965, 4, 2401–2411.
- (14) Edelhoch, H. *Biochemistry* 1967, 6, 1948–1954.
- (15) Crimmins, D.; Isom, L.; Holtzer, A. *Comp. Biochem. Physiol.* 1981, 69B, 35–46.
- (16) Betteridge, D.; Lehrer, S. *J. Mol. Biol.* 1983, 167, 481–496.
- (17) Edwards, B.; Sykes, B. *Biochemistry* 1980, 19, 2577–2583, especially Table I.
- (18) Mattice, W., personal communication (1980).

Halato-Telechelic Polymers. 10. Effect of the Ionic End Groups on the Glass Transition Temperature

R. JÉRÔME,* J. HORRION, R. FAYT, and PH. TEYSSIE

Laboratory of Macromolecular Chemistry and Organic Catalysis, University of Liège, Sart-Tilman 4000, Liège, Belgium. Received March 23, 1984

The incorporation of ions induces drastic modifications in the physicochemical properties of organic polymers.^{1–3} The obvious technical importance of the subject has promoted an in-depth investigation of both the supermolecular structure and the thermal transitions of ion-containing polymers and, more especially, of ionomers. It is worth recalling that ionomers usually result from the incorporation of relatively few ionic groups into nonpolar polymers by the random copolymerization of common organic monomers with ionizable comonomers.

Eisenberg³ has reviewed the effect of ions on the glass transition temperature (T_g) of ionomers based mainly on styrene,⁴ butadiene,⁵ ethyl acrylate,⁶ and ethylene.⁷ The glass transition temperature increases with increasing salt (metal acrylate or methacrylate) content and, although no meaningful correlation exists as yet, the effect would seem more pronounced as the T_g of the host material decreases.³ Some experimental results⁸ support that cross-linking by

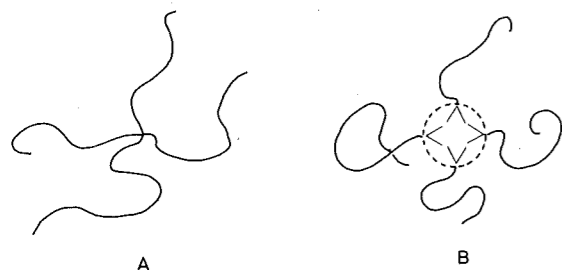


Figure 1. Schematic illustration of polymers cross-linked through covalent bonds (A) and ionic aggregates (B). For convenience, the ionic aggregates are pictured as spherical multiplets without presuming their actual nature and geometry. The packing density of the chain segments is increased at the cross-links of A-type polymers, whereas it is largely reduced at the surface of the ionic aggregates (B-type polymers).

anionic species is a mechanism for raising T_g , whereas other ones⁷ agree rather well with values predicted by a copolymerization equation. It is likely that both cross-linking and a copolymerization effect play a role in fixing the T_g of ionomers. The effectiveness of various ions in raising the glass transition temperature depends on the q/a ratio (electrostatic field), where q is the counterion charge and a the distance between the centers of the charges in the contact ion pair.⁶ Finally, the degree of clustering of the ions, particularly at moderately high ionic concentrations, can also decrease segmental mobility sufficiently to have an appreciable effect on T_g . The T_g 's of styrene and ethyl acrylate ionomers show meaningful changes in slope when plotted as a function of the ionic comonomer content.^{6,9} Below a given content, the initial rise in T_g is linear and attributed to the ion aggregation into small tight multiplets. Above that concentration, the rate of increase accelerates and is supposed to reflect the onset of clustering. The rather complex behavior of ionomers makes these compounds evidently unsuitable for an unambiguous approach of the effect of ions attached onto polymeric backbones. This is why an extensive study of model ion-containing polymers, i.e., halato-telechelic polymers (HTP), has been recently undertaken:¹⁰⁻¹⁶ while the ionic groups are more or less randomly distributed as pendant groups in ionomers, they are selectively attached at both ends of linear chains in HTP.

Polydiene-based HTPs have been largely investigated up to now, and the neutralization of α,ω -dicarboxylatopolybutadiene ($\bar{M}_n = 4600$) with divalent metal has no detectable effect on T_g .¹⁵ On the other hand, the dynamic mechanical properties of α,ω -alkaline earth dicarboxylatopolybutadiene^{11,15} and -polyisoprene¹⁶ show unambiguously that the ionic end groups aggregate and give rise to a relaxation mechanism obeying an Arrhenius-type temperature dependence. In the glass transition region of polybutadiene (193 K), the ionic aggregates may be represented as stable cross-links. At low temperature, the relaxation time (τ_m) of the ion pair interactions is likely to be longer than the time required for the glass transition detection (t). No modification of the ionic aggregates is therefore observable in time and they behave as permanent tie points of the chains. It is well-known that the chemical (sulfur, peroxide, etc.) cross-linking of polymers restrains the chain mobility (or reduces the free volume; Figure 1A), resulting in the effective raising of T_g . When attached at the surface of large and stable ionic aggregates, the chain ends suffer also a loss of mobility, the effect of which might however be counterbalanced by a decrease in their packing density. Indeed, because of the steric hindrance between metal carboxylate groups, the chain-end overlap is expected to be markedly reduced and to create extra free

volume (Figure 1B). Conclusively, it is believed that the insensitivity of T_g of polybutadiene to the presence of metal carboxylate end groups results from the annihilation of two opposite effects, i.e., restriction of chain-end mobility and reduced crowding at the branch points.

Recent Observations

A quite different behavior is observed when α,ω -dicarboxylatopolystyrene ($\bar{M}_n = 22000$) is neutralized with alkali metal and alkaline earth cations (Table I). The glass transition temperature of the neutralized polymer is markedly less than that of the carboxylic acid form (365 K). Also the size of the specific cation employed markedly affects the T_g with the largest cations having the lowest T_g for both the alkali metal and alkaline earth series. When neutralization is performed simultaneously with two different alkaline earth cations, i.e., Ba^{2+} ($W_{\text{Ba}} = 0.38$) and Mg^{2+} ($W_{\text{Mg}} = 0.62$), the experimental T_g (313 K) obeys Fox's relationship (312 K)

$$\frac{1}{T_{g_{\text{Ba,Mg}}}} = \frac{W_{\text{Ba}}}{T_{g_{\text{Ba}}}} + \frac{W_{\text{Mg}}}{T_{g_{\text{Mg}}}}$$

where $T_{g_{\text{Ba}}}$, $T_{g_{\text{Mg}}}$, and $T_{g_{\text{Ba,Mg}}}$ are the T_g of the polymer neutralized with Ba, Mg, and a mixture of Ba and Mg, respectively, and W_{Ba} and W_{Mg} are the weight percent of polystyrene neutralized with Ba and Mg, respectively. The neutralization was achieved as described elsewhere;¹³ it proceeded in dry toluene through addition of the due amount of barium methoxide and magnesium methoxide to the carboxy-telechelic polybutadiene. Complete reaction was ensured by distilling off the formed methanol. The neutralization of α,ω -dicarboxylatopoly(α -methylstyrene) ($\bar{M}_n = 10000$) is responsible for a relatively less important depression of T_g than that due to polystyrene (Table II). Again, Ba^{2+} is more efficient than Mg^{2+} . Furthermore, the T_g of the neutralized polymer is always lower when it is measured simply after neutralization, solvent removal, and drying up to constant weight (25 °C, 10^{-4} torr), rather than after compression molding of the bulk HTP (Table II). It is however noteworthy that after an annealing at 200 °C for 30 min the nonmolded samples exhibit practically the same T_g as that observed after compression molding.

Discussion and Conclusions

As ion pair interactions are governed by an Arrhenius-type activation process,¹⁵ the ion aggregation is expected to decrease when temperature increases. In the glass transition region of polystyrene ($T_g = 365$ K) and poly(α -methylstyrene) ($T_g = 427$ K), τ_m could be assumed shorter than t , and scrambling of the ionic aggregates would already occur in the polymeric matrix near T_g . In that temperature range, the polystyrene and poly(α -methylstyrene) chain ends would not be permanently attached at the surface of stable particles but would exchange more or less easily. The decrease in T_g could be a result of the increased mobility of the chain ends combined with more free volume around branching points. In order to account more accurately for the experimental results, the thermal dependence of the ion aggregation process must be discussed. At low temperatures, the ionic aggregates are stable ($\tau_m \gg t$) and their size is the largest (Figure 2A). As temperature increases, τ_m decreases to become finally shorter than t , and the ion pairs in the aggregates exchange faster. The temporarily free ion pairs and/or small-size multiplets can either move within the aggregate or diffuse into surrounding ones. As charge separation requires a prohibitive energy in nonpolar media, the diffusing species in alkaline earth dicarboxylato polymers are likely triplet

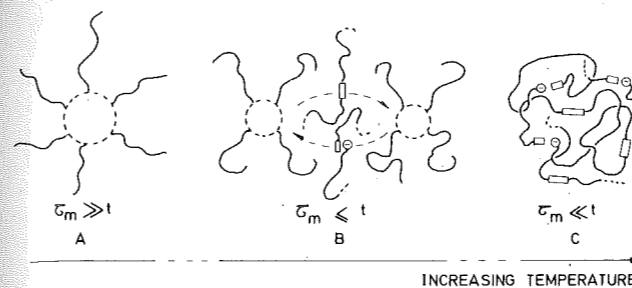


Figure 2. Thermal dependence of the aggregation of alkaline earth carboxylates in a viscous nonpolar polymer matrix: (A) stable ionic aggregates; (B) dynamic equilibrium between scrambled aggregates and diffusing small-size multiplets ($\sim\sim\sim\text{O}\sim\sim\sim$ is a triplet, and $\sim\sim\sim\text{O}\sim\sim\sim$ is [doublet + free anion]); (C) completely dissociated ionic aggregates. τ_m is the relaxation time of the ion pair interactions and t the time required for the glass transition detection.

Table I
Effect of Neutralization on T_g^a of
 α,ω -Dicarboxylatopolystyrene^b ($\bar{M}_n = 22000$)

cation	ionic radius, Å	T_g , K
Li	0.68	365
K	1.33	300
Mg	0.66	321
Ba	1.34	298
Ba (0.38) + Mg (0.62)		313

^a T_g was measured with the Du Pont 990 thermal analyzer (heating rate 20 °C·min⁻¹). The samples were compression molded at 150 °C and slowly cooled to 25 °C (≈ 30 min) before characterization. The T_g values were quite reproducible when the measurements were repeated after the slow cooling of the sample from 150 °C (≈ 5 °C·min⁻¹). ^b The carboxy-telechelic polystyrene was anionically prepared in THF at -78 °C, with the tetramer of α -methylstyrene sodium as initiator. The living macrodianions were deactivated by excess anhydrous carbon dioxide.

[$\sim\sim\sim\text{COOMeOOC}\sim\sim\sim$] and/or doublet + anion [$\sim\sim\sim\text{COOMe}^+\text{OOC}\sim\sim\sim$]. A dynamic equilibrium can take place between diffusing multiplets and ionic aggregates (Figure 2B), which depends on the temperature (thermodynamic control) and the viscosity of the polymeric matrix (kinetic control). At very high temperatures, the occurrence of the smallest multiplets is favored (Figure 2C).

The main experimental results reported in Tables I and II may be now discussed referring to Figure 2. When the polymer is molded (423 or 473 K), the ions aggregate in the melt and the process extends as temperature decreases down to T_g , as illustrated from Figure 2C to Figure 2B. Molded halato-telechelic polystyrenes which have a lower T_g contain bigger aggregates than molded halato-telechelic poly(α -methylstyrenes). From Tables I and II, the T_g depression obviously increases in the same way. Furthermore, the ion aggregation process must be more important in samples prepared by solvent removal at 298 K than in those obtained by compression molding above T_g . Table II shows that T_g is once more deeply depressed in the former. That effect is however not noticeable for halato-telechelic polystyrene, the T_g of which is very close to 298 K, i.e., the temperature at which the neutralized polymer is recovered from solution before molding (Table I, third column). That different behavior of polystyrene and poly(α -methylstyrene) suggests that the presence of solvent remaining in the samples after drying is unlikely and cannot explain the changes in T_g induced by the molding of halato-telechelic poly(α -methylstyrenes). Previous investigations have shown that the bigger the cation is, the larger the mean size of the ionic aggregates is.¹⁵ That behavior agrees well with the higher effective-

Table II
Effect of Neutralization on T_g of
 α,ω -Dicarboxylatopoly(α -methylstyrene)^a ($\bar{M}_n = 10000$)

cation	T_g , K	
	before molding	after molding at 200 °C
	427	427
Mg	363 ^b	409
Ba	359 ^b	388

^a The experimental conditions are the same as described for Table I. ^b After an annealing at 200 °C, T_g tends to the value observed for the sample molded at 200 °C.

ness of Ba^{2+} and K^+ compared to Mg^{2+} and Li^+ , respectively. Conclusively, a correlation between the T_g depression and the mean size of the ionic aggregates emerges clearly. That experimental observation may be accounted for if the free volume of the aggregates is assumed to be higher than that of the polymer matrix. The free volume of the polymer would increase proportionately to the extent of the ion aggregation. This is supported in part by the increase in both the free volume fractions at 298 K (f_{298}) and the volume expansion coefficient (α_f) of α,ω -dicarboxylatopolyisoprenes (\bar{M}_n ranging from 20000 to 70000) upon neutralization by magnesium methoxide.¹⁶ When τ_m is shorter than t , the excess of free volume in the ionic aggregates can, at least partly, be yielded to the polymer segments. Finally, the molding of HTPs, with a glass transition in the temperature range of Figure 2C, is expected to have little effect on T_g . No ionic aggregate is formed in the polymer and the mobility of the chain ends is weakly depressed by their attachment to largely free ion pairs (doublet + free anion) and/or triplets which exchange continuously through an ion-hopping process.

The apparent validity of Fox's relation when Ba and Mg are simultaneously used to neutralize α,ω -dicarboxylatopolystyrene (Table I) would mean that the free volume contribution of each type of metal carboxylate aggregates adds to each other.

As already stressed, halato-telechelic polymers are attractive materials to study the role of the ions in the aggregation mode and of its consequences on the physico-mechanical properties. If the decrease of T_g (initially located around 373 K) may really be related to the average size of the ionic aggregates, it is an easy way to compare the effectiveness of different ion pairs to aggregate and to estimate the effect of various preparation techniques and posttreatments on that process.

Further work is in progress to elucidate this unexpected "plastification effect" in thermoplastics modified by ionic end groups able to increase the free volume through dynamic interactions.

Acknowledgment. We are indebted to the "Services de la Programmation de la Politique Scientifique" (Brussels) for support of this work.

References and Notes

- Otocka, E. P. *J. Macromol. Sci., Rev. Macromol. Chem.* **1971**, C5, 275.
- Holliday, L., Ed. "Ionic Polymers"; Applied Science Publishers: London, 1975.
- Eisenberg, A.; King, M. "Polymer Physics"; Stein, R. S., Ed.; Academic Press: New York, 1977; Vol. 2.
- Eisenberg, A.; Navratil, M. *Macromolecules* **1974**, *7*, 90.
- Otocka, E. P.; Eirich, F. R. *J. Polym. Sci., Part A-2* **1968**, *6*, 921.
- Mastuura, H.; Eisenberg, A. *J. Polym. Sci., Polym. Phys. Ed.* **1976**, *14*, 773.
- Otocka, E. P.; Kwei, T. K. *Macromolecules* **1968**, *1*, 401.
- Ogura, K.; Sobue, H.; Nakamura, S. *J. Polym. Sci., Polym. Phys. Ed.* **1973**, *11*, 2079.
- Eisenberg, A. *Contemp. Top. Polym. Sci.* **1979**, *3*, 231.

- (10) Broze, G.; Jérôme, R.; Teyssié, Ph. *Macromolecules* 1981, 14, 224.
 (11) Broze, G.; Jérôme, R.; Teyssié, Ph.; Marco, C. *Polym. Bull.* 1981, 4, 241.
 (12) Broze, G.; Jérôme, R.; Teyssié, Ph.; Gallot, B. *J. Polym. Sci., Polym. Lett. Ed.* 1981, 19, 415.
 (13) Broze, G.; Jérôme, R.; Teyssié, Ph. *Macromolecules* 1982, 15, 920.
 (14) Broze, G.; Jérôme, R.; Teyssié, Ph. *Macromolecules* 1982, 15, 1300.
 (15) Broze, G.; Jérôme, R.; Teyssié, Ph.; Marco, C. *J. Polym. Sci., Polym. Phys. Ed.* 1983, 21, 2205.
 (16) Broze, G.; Jérôme, R.; Teyssié, Ph.; Marco, C. *Macromolecules* 1983, 16, 1771.

Density Profiles of Polymer-Containing Nuclei

YITZHAK RABIN[†] and HOWARD REISS^{*}

Department of Chemistry and Biochemistry, University of California, Los Angeles, Los Angeles, California 90024.

Received March 26, 1984

In a recently reported experiment, gas-phase polymerization was successfully demonstrated in supersaturated monomer vapor.¹ Due to the sharp threshold behavior of the nucleation process, once the polymer grows to a certain critical size it serves as a nucleus for inhomogeneous nucleation of vapor monomers, and the resulting polymer-containing droplet condenses out of the vapor. The critical droplet was analyzed in the framework of a surface-modified, Flory-Huggins-type model,² which gave the polymer size dependence of the nucleation barrier and the effective surface tension of the droplet.³

In this note we present a model for density profiles of polymer-containing droplets, accounting for polymer chain connectivity and finite droplet size effects. The model combines a modified version of the lattice-fluid (LF) theory⁴ with the self-consistent field (SCF) theory of polymer chains in solvents.⁵⁻⁷

The model is of some general interest, since the problem does not seem to have been addressed previously, although studies of the interface between a bulk polymer solution and its vapor have been performed. The present problem is not only of interest to the theory of nucleation but also to the field of air pollution, where very small particles of polymer solution may be in quasi-equilibrium with ambient vapors (although in this case we are concerned with "stable" rather than "unstable" equilibrium).

Neglecting the polymer entropy of mixing term (a single polymer inside a droplet) and assuming equilibrium between monomers in the droplet and in the surrounding vapor, the square-gradient approximation to the chemical potential gives⁴⁻⁷

$$-\left(\frac{\partial^2}{\partial r^2} + \frac{2\partial}{r\partial r}\right)\rho(r) - 2(\rho(r) - \rho(\infty)) + T\left(\frac{1}{l_m} \ln \frac{\rho_m(r)}{\rho(\infty)} - \ln \frac{1 - \rho(r)}{1 - \rho(\infty)}\right) = 0 \quad (1)$$

where we assume that the monomer and polymers differ only in their length parameters (l_m and $l_p \gg l_m$, respectively⁸) and that the droplet is spherically symmetric. Also, $\rho(r) = \rho_m(r) + \rho_p(r)$, $\rho_m(r)$ ($\rho_p(r)$) being the local monomer (polymer) density. The distance r and temperature T are scaled in appropriate units.⁸

Using the SCF theory of polymer chains, in the long-chain limit⁶ we obtain $\rho_p(r) = (N_p/4\pi)(\psi^2(r)/r^2)$, where N_p

[†] Present address: Center for Studies of Nonlinear Dynamics, La Jolla Institute, La Jolla, CA 92037.

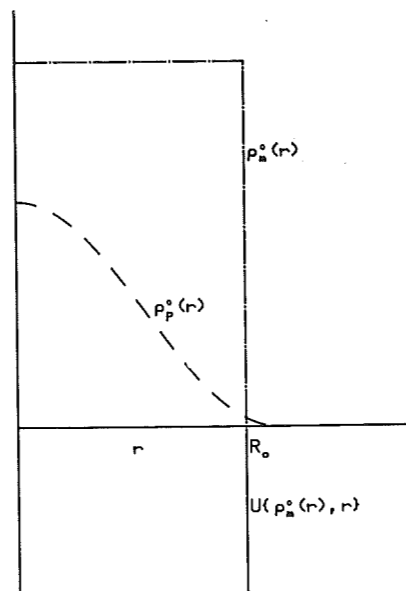


Figure 1. Solvent density profile $\rho_m^{(0)}(r)$ (---) and the corresponding SCF potential $U[\rho_m^{(0)}(r), r]$ (—). The resulting polymer density profile $\rho_p^{(0)}(r)$ is given by the dashed line.

is the number of statistically independent polymer chain segments (each of length b_p) and $\psi(r)$ is the normalized eigenfunction corresponding to the lowest eigenvalue (E_0) of the Schrödinger-like equation

$$\left(-\frac{b_p^2}{6} \frac{\partial^2}{\partial r^2} + U[\rho_m(r), \rho_p(r)]\right)\psi(r) = E_0\psi(r) \quad (2)$$

subject to the boundary conditions

$$\frac{\partial}{\partial r} \left(\frac{\psi}{r}\right) \Big|_{r=0} = 0; \quad \psi(\infty) = 0$$

The SCF potential $U[\rho_m, \rho_p]$ is given by

$$U[\rho_m(r), \rho_p(r)] = -\left(\frac{\partial^2}{\partial r^2} + \frac{2}{r} \frac{\partial}{\partial r}\right)\rho(r) - 2(\rho(r) - \rho(\infty)) - T \ln \frac{1 - \rho(r)}{1 - \rho(\infty)} \quad (3)$$

For a given temperature (T) and monomer pressure (determining $\rho(\infty)$), eq 1-3 can be solved numerically, resulting in the density profile $\rho_p(r)$, $\rho_m(r)$.⁹ Here, we present a semianalytical solution for the case of a large, polymer-dilute droplet (small polymer volume fraction). We try an iterative solution, first using eq 1 with $\rho_p(r) = 0$ to obtain the density profile $\rho_m^{(0)}(r)$ of a homogeneous critical nucleus with radius R_0 , and then compute the SCF potential $U[\rho_m^{(0)}(r), 0]$ and use it to solve eq 2 for the polymer density profile $\rho_p^{(0)}(r)$. The latter is then used in eq 1 to compute a corrected value for the monomer density profile ($\rho_m^{(1)}(r)$) and the iteration continues until convergence is obtained.

Taking $\rho_m^{(0)}(r) = \rho_m^{(0)}(0)\theta(R_0 - r)$, where θ is the theta function, the SCF potential has a "square well" form (Figure 1). Application of the variation method¹⁰ gives

$$\rho_p^{(0)}(r) = \frac{2\pi^2}{3} \left(1 - \frac{3\delta}{\pi}\right) \frac{N_p}{(4\pi/3)R_0^3} \frac{\sin^2[\pi(1 - \delta/\pi)(r/R_0)]}{[\pi(1 - \delta/\pi)(r/R_0)]^2}, \quad r \leq R_0 \quad (4a)$$

$$\rho_p^{(0)}(r) = \frac{2}{3} \delta^2 \frac{N_p}{(4\pi/3)R_0^3} \frac{e^{-2\pi\delta(r-R_0)/R_0}}{(r/R_0)^2}, \quad r \geq R_0 \quad (4b)$$

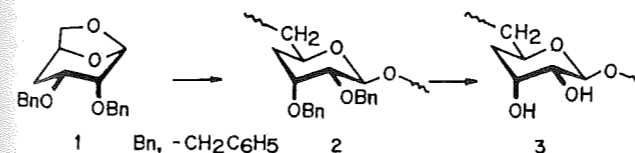
where we include lowest order corrections in $\delta = (\pi/3)(b_p/R_0)[l_m/(2|\ln \rho(\infty)|)]^{1/2}$. Estimating the experimentally controlled parameters, $T \approx 0.5$, $l_m \approx 10$, $\rho_m(0)/\rho_m(\infty) \approx 300$, we find that the solutions converge rapidly (i.e., are close to $\rho_p(0)$ and $\rho_m(0)$) provided that the polymer volume fraction in the nucleus, $N_p/(4\pi/3)R_0^3\rho_p^*$, is much smaller than 0.15 (ρ_p^* is the close-packed polymer density). Corrections lead to a slight increase of size of the critical droplet due to chain penetration into the droplet-vapor interface driven by entropy of confinement effects⁶ (of order $(b_p/R_0)^2$).

We conclude this note by commenting on an interesting aspect of polymer growth in supersaturated vapor. In the absence of nucleation, low temperature and polymer concentration will lead to a collapsed (globular) state of the polymer chain.⁶ However, once enough monomers are adsorbed on the polymer, the critical droplet size is reached and the droplet proceeds to grow to macroscopic dimensions. The polymer chain expands inside the droplet until the swollen configuration corresponding to a polymer in good solvent is reached. Thus, the nucleation process is accompanied by the globule-to-coil transition of the polymer.

Communications to the Editor

Chemical Synthesis of Polysaccharides. 4. 4-Deoxy-(1→6)-β-DL-ribo-hexopyranan, the First Example of a (1→6)-β-Linked Polysaccharide Synthesized by the Ring-Opening Polymerization Method

In recent years, a variety of polysaccharides and their analogues have been synthesized by the cationic ring-opening polymerization of anhydrosugar derivatives.¹⁻⁶ Above all, the polymerization of 1,6-anhydrosugar derivatives has been most extensively investigated, since it often yields high molecular weight stereoregular polymers exclusively composed of (1→6)-α-pyranosyl residues under appropriate reaction conditions, particularly at low temperatures. With the rise in polymerization temperature, the stereoregularity of the polymers is generally lost because of the concomitant formation of (1→6)-β-pyranosyl residues along with the predominant (1→6)-α-pyranosyl residues.⁷ To the best of our knowledge, there has been no publication dealing with the chemical synthesis of polysaccharides predominantly or exclusively consisting of (1→6)-β-pyranosyl residues from 1,6-anhydrosugar derivatives. In the present communication, we report the chemical synthesis of 4-deoxy-(1→6)-β-DL-ribo-hexopyranan (3) by the ring-opening polymerization of a bicyclic acetal (1) derived from noncarbohydrates sources, followed by debenzoylation of the resulting polymer (2).⁸ This is the first example of a regularly (1→6)-β-linked polysaccharide obtained by the ring-opening polymerization method.



Monomer 1, 3(e),4(a)-bis(benzyloxy)-6,8-dioxabicyclo-

Acknowledgment. Although the information in this document has been funded by the U.S. Environmental Protection Agency under assistance agreement CR 807864-02-0 to the National Center for Intermedia Transport Research, it does not necessarily reflect the views of the Agency, and no official endorsement should be inferred.

References and Notes

- M. A. Chowdhury, H. Reiss, D. R. Squire, and V. Stannett, *Macromolecules*, 17, 1436 (1984).
- P. J. Flory, "Principles of Polymer Chemistry", Cornell University Press, Ithaca, NY, 1953.
- H. Reiss and M. A. Chowdhury, *J. Phys. Chem.*, 87, 4599 (1983).
- I. C. Sanchez, *J. Macromol. Sci., Phys.*, B17, 565 (1980).
- E. Helfand and A. M. Sapse, *J. Polym. Sci., Polym. Symp.*, No. 54, 289 (1976).
- I. M. Lifshitz, A. Y. Grosberg, and A. R. Khokhlov, *Rev. Mod. Phys.*, 50, 683 (1978).
- K. M. Hong and J. Noolandi, *Macromolecules*, 14, 1223 (1981).
- I. C. Sanchez and R. H. Lacombe, *J. Phys. Chem.*, 80, 2352 (1976).
- Y. Rabin and M. A. Chowdhury, to be published.
- L. I. Schiff, "Quantum Mechanics", 3rd ed., McGraw-Hill, New York, 1955.

[3.2.1]octane (1,6-anhydro-2,3-di-O-benzyl-4-deoxy-β-DL-ribo-hexopyranose), was synthesized from 3,4-dihydro-2H-pyran-2-carbaldehyde (acrolein dimer) via five reaction steps: The precursor of 1, 3(e),4(a)-dihydroxy-6,8-dioxabicyclo[3.2.1]octane, was prepared by the procedures described by Brown et al.⁹⁻¹¹ with some modifications. Subsequent benzylation of the dihydroxy compound by the conventional method using sodium hydride and benzyl chloride in dimethyl sulfoxide gave monomer 1 as white crystals. The monomer was purified by recrystallization three times from ethanol and finally from a mixture of *n*-hexane and dichloromethane (2.5:1 volume ratio): mp 42.5-43.5 °C; ¹³C NMR (CDCl₃, 50 MHz, Me₄Si) δ 138.34 and 138.17 (phenyl (ipso)), 128.18 (phenyl (meta)), 127.73 (phenyl (para)), 127.39 and 127.19 (phenyl (ortho)), 100.51 (C(5)), 73.74 (C(3)), 72.91 (benzyl), 71.94 (C(4)), 71.10 (C(1)), 70.31 (benzyl), 66.81 (C(7)), 32.47 (C(2)) (the numbering is based on the IUPAC nomenclature of organic chemistry). Anal. Calcd for C₂₀H₂₂O₄: C, 73.60; H, 6.79. Found: C, 73.71; H, 6.80.

Polymerization of 1 was carried out in three different solvents, toluene, dichloromethane, and 1-nitropropane, with phosphorus pentafluoride as initiator at -60 °C. A high-vacuum technique was employed for the polymerization. A polymer was separated from the reaction mixture by repeated reprecipitation using dichloromethane and methanol as a solvent-precipitant pair, followed by freeze-drying from a benzene solution. The results of the polymerization are presented in Table I.

The polymer prepared in toluene showed a higher melting point (Table I) and lower solubility than the polymers obtained in the other two solvents: The former polymer was soluble in benzene, chloroform, dichloromethane, 1,2-dimethoxyethane, and pyridine and insoluble in 1,4-dioxane, dimethylformamide, 1-nitropropane, and toluene, whereas the latter polymers were soluble in all these solvents. Such remarkable differences conceivably